Separation and Purification Technology 168 (2016) 141–151

Contents lists available at ScienceDirect

Separation and Purification Technology

journal homepage: www.elsevier.com/locate/seppur

Pervaporation of ammonia solution with γ-alumina supported organosilica membranes

Xing Yang [a,b,*], Lining Ding [a,b], Martin Wolf [c], Frans Velterop [c], Henny J.M. Bouwmeester [d], Simon Smart [e], João C. Diniz da Costa [e], Audra Liubinas [f], Jun-De Li [b], Jianhua Zhang [a,b], Mikel Duke [a,b,*]

[a] Institute for Sustainability and Innovation, College of Engineering and Science, Victoria University, P.O. Box 14428, Melbourne, Victoria 8001, Australia
[b] School of Engineering and Science, Victoria University, Werribee 3030, Victoria, Australia
[c] Pervatech, The Netherlands
[d] Inorganic Membranes, University of Twente, The Netherlands
[e] The University of Queensland, FIM²Lab – Functional Interfacial Materials and Membranes Laboratory, School of Chemical Engineering, Brisbane, Qld 4072, Australia
[f] City West Water, Melbourne, Victoria 3020, Australia

ARTICLE INFO

Article history:
Received 19 February 2016
Received in revised form 15 May 2016
Accepted 17 May 2016
Available online 18 May 2016

Keywords:
Molecular sieve
Organosilica membrane
Pervaporation
Separation factor
Enhanced transport mechanism

ABSTRACT

In this work, pervaporation of ammonia-solution using γ-alumina supported organosilica membrane (HybSi®, Pervatech) was explored to understand ammonia removal performance and material stability in this unique high pH environment. During the testing of synthetic ammonia solution of 50 mg/L at 45 °C (pH 10), the hybrid silica membrane showed a preference towards ammonia transport over water, with an ammonia separation factor up to 12 and flux of 4.3 kg m^{-2} h^{-1} stable in a continuous testing period of 7 h. At an ammonia concentration of 1000 mg/L (pH 11), the membrane initially exhibited separation preference towards ammonia at 45 °C, then gradually reversed to water selective after increasing to 70 °C, where a significant flux decline was observed. The membrane degradation was investigated by FTIR, porosimetry, SEM and XRD. Only slight change in organosilica chemistry and structure was evident, however more significant degradation was observed in the supporting γ-alumina layer. The changes in crystalline alumina structure, porous properties and physical structure undermined the functional silica separation layer. Therefore while the organosilica membrane appeared stable in the high pH aqueous ammonia environment, membranes for ammonia pervaporation applications should consider alternative supporting layers to γ-alumina.

1. Introduction

The presence of nitrogen compounds in the natural waterways is hazardous, particularly if it is in volatile (e.g., ammonia) forms. The excessive ammonia in water is known to cause eutrophication and hence harmful to aquatic life [1–3]. Also, ammonia in volatile form (at its native high pH) can be trapped in sewer headspaces presenting a safety issue to workers. Thus, ammonia nitrogen must be removed by water treatment plants (e.g., aerobic biological processes), which however require a large amount of energy and cost. Alternatively, the ammonia nitrogen could be stripped and broken down/converted more efficiently, or potentially concentrated for recycling as a valuable product to avoid expensive treatment and environmental hazards.

Since the 1980s membrane-based gas adsorption/stripping processes have been widely employed to remove ammonia from industrial wastewater, however the low efficiency with respect to energy consumption and costly regeneration processes have limited its applications for treating feeds with a wide range of concentrations [4]. Recently, ammonia removal using vacuum membrane distillation (VMD) was proposed as a low cost and simple technology without chemical addition [5–7]. About 90% ammonia removal was achieved using highly permeable polytetrafluoroethylene (PTFE) hydrophobic membranes in VMD, with an ammonia separation factor of 3–8 at pH ~13. Similarly, a solution of 1000 mg/L ammonia concentration was concentrated to 12,000 mg/L in VMD using polypropylene (PP) hollow fiber membranes [7], which has met the minimum target value for on-site reuse. Nevertheless, given the difficulty of separating the ammonia-water system above its inherent thermodynamic limits, the existing MD processes are still restricted from achieving high separation efficiency in one step. Also, organic fouling and membrane wetting becomes a critical issue for hydrophobic membrane

* Corresponding authors at: College of Engineering and Science, Victoria University, P.O. Box 14428, Melbourne, Victoria 8001, Australia.
E-mail addresses: xing.yang@vu.edu.au (X. Yang), mikel.duke@vu.edu.au (M. Duke).

http://dx.doi.org/10.1016/j.seppur.2016.05.017
1383-5866/

Nomenclature

A	specific surface area, m^2/g
c	concentration of a component in the aqueous solution, mg/L
d_p	pore size, nm
p	absolute pressure at gas physisorption, kPa
p_0	saturation pressure of gas at temperature T_0, MPa
Q_f	feed flow rate, L min^{-1}
T_f	bulk temperature of the feed, K

Greek letters

α	membrane permselectivity
β	separation factor of ammonia
λ	wavelength
θ	angle of diffraction, °

Suffix

H_2O/NH_3	water over ammonia
f	feed
p	permeate

applications in treating challenging feeds [8]. Therefore, a more effective membrane process with highly selective membranes is required to recover ammonia from waste water of various characteristics, e.g., ammonia concentration, pH and turbidity.

Alternatively, molecular separation using pervaporation with nanostructured membranes has become an energy-saving option for the separation of challenging binary or multi-components, particularly in the areas of gas separation [9], biofuel and solvent dehydration where water is the minor component [10]. In recent years, the application of molecular sieve silica membranes has been extended to water treatment industry [11,12] and in 2007 was first introduced to pervaporative desalination [11], where water vapour selectively diffused through the silica matrix while salts were rejected. In order to achieve this, water stable silica materials were used since amorphous microporous silica membranes are known to be unstable at high temperatures in the presence of water vapour, which causes densification of the silica network and generates mobile silanol groups (Si—O—Si) due to hydrolysis reaction [13–15]. Subsequently, the widening of large pores and collapse of small pores in the silica structure caused by the migration of mobile silanol groups would result in performance loss [16]. Different approaches have been proposed for improving the hydrothermal stability of silica-based ceramic membranes such as carbonized templating [16–21], metal oxide doping [22,23] and organic-inorganic hybrid silica [24,25]. It was reported that the metal oxide doped silica membrane exhibited excellent durability in desalination application up to 570 days without flux decline and performance deterioration [22]. With such advances in silica material hydrostability, attention can now be paid to more diverse systems such as those which contain ammonia.

For the application of ammonia capture or stripping, molecular sieve silica structures can separate based on physical size exclusion and adsorption phenomena. The molecular size difference between smaller water (kinetic diameter of 0.26 nm [26]) and larger ammonia molecules (estimated kinetic diameter 0.26 [26] or 0.326 nm [27]) suggest a material that would give preference to diffusing water molecules over ammonia. However at the same time, there is a strong adsorption between silica and ammonia which competes against water if ammonia can enter the silica micropores. The competing size exclusion and adsorption between water and ammonia in silica-based microporous materials is already well-known, and has shown ammonia selectivity over hydrogen in gas phase due to the natural adsorption affinity in the tight pore spaces [9,28,29]. It is therefore viable, but still a new concept in membrane research for fabricating suitable membranes to separate ammonia from aqueous solution. A novel method was proposed [7] to capture ammonia using a cobalt-doped molecular sieve silica membrane in pervaporation, which demonstrated exceptional ammonia selectivity up to 60, which was 5-fold more effective than that of polymer membranes working according to distillation. However, rapid material degradation was observed in few hours. Therefore in order to explore the role of hydrostable silica membranes in ammonia capture and stripping applications, a study on the mechanism of material degradation in the presence of ammonia solutions is needed. In recent decades, the rapid development of organic–inorganic hybrid silica membranes with controllable pore size has become a promising area for separations involving water. The introduction of organic fragments in the silica network by using bis-silyl precursors makes the membrane resilient to high temperature and tough aqueous environment without losing separation function, which was demonstrated by Pervatech, the Netherlands, in long-term alcohol dehydration processes [17,24,30]. Only in recent years such hybrid silica membranes have been applied in other aqueous environments, *i.e.,* in 2011 an organosilica membrane with bis (triethoxysilyl) methane (BTESM) precursor was designed [31] for RO applications and demonstrated exceptional hydrothermal stability as well as molecular sieving properties. Hybrid silica membranes were reported to have stability issues with acidic feeds over certain limits [30] but have never been applied in alkaline conditions, such as ammonia solution. Further, silica membranes have been prepared on γ-alumina support layers as it provides a smooth and suitably staged pore size reduction from the macroporous α-alumina substrate. Despite the importance of this layer supporting silica thin films, little attention has been paid to its role in membrane stability. Therefore a study on the composite organosilica/γ-alumina membrane performance followed by material changes of the membrane and individual materials in the presence of the more aggressive ammonia and high pH environment is the focus of this research.

2. Experimental

2.1. Membrane material

Organic-inorganic hybrid silica-based ceramic membranes HybSi® were provided by Pervatech, the Netherlands. This tubular membrane consists of three layers: (1) support layer: macroporous α-Al_2O_3 layers; (2) intermediate layer: mesoporous γ-Al_2O_3 layer; (3) coating layer: molecular sieve organosilica silica. As described in previous work [32], the mesoporous γ-Al_2O_3 layers were prepared by a dip-coating procedure using a boehmite sol on a 10-cm long tubular macroporous α-Al_2O_3 tube (obtained commercially from Inopor). The hybrid silica layer was coated using the hybrid silica sol prepared from bis-silyl precursor BTESM (*i.e.,* $(EtO)_3Si—CH_2—Si(OEt)_3$). The sol deposition was done by a dip coating technique on the inner surface of the tubes under class

1000 clean room conditions to minimise defect formation due to dust particles. The tubes have an inner diameter of 7 mm, and were calcined at 300 °C for 2 h in a nitrogen flow (99.999% pure), applying heating and cooling rates of 0.5 °C/min [32]. The silica top layer exhibits hydrophilic surface properties and a narrow pore size distribution with pore size between 0.3 and 0.5 nm as measured by permporometry [30].

2.2. Membrane performance tests

Pervaporation experiments were performed using a bench-top setup, as shown in Fig. 1, in which a stainless steel tubular module containing one HybSi® tube was installed. Two identically-made membranes #1 and #2 were tested for repeatability purposes. For each PV test, the membrane tube, with a length of 70 mm and inner surface area of 0.0022 m^2, was sealed in the membrane module using rubber O-rings. As the membrane is coated on the inner surface, the feed mixture was circulated continuously through the tube side of the module by a peristaltic pump (500 mL min^{-1}); the permeate was collected at the shell side (in contact with the porous support of membrane) with a vacuum (100–450 Pa) applied by an oil pump. Feed solution mixing was controlled using a stirrer bar with a speed of 500 rpm and heated to the desired test temperature between 35 and 70 °C. Two cold traps containing liquid nitrogen were placed along the vacuum line to capture the vapour generated. The product was collected and measured at 30 min intervals in the first trap. The second trap simply offered protection for the oil diaphragm pump from corrosion caused by uncondensed volatiles. During batch operation with small membrane area, the feed concentration was maintained constant by continuously supplying fresh feed. Permeate samples were collected after an initial 5-min evacuation under VMD mode, to eliminate the effect of adsorbed ammonia in the silica material that might have occurred upon the initial contact of the membrane with the feed solution. Also, the membrane was completely removed from the ammonia solution and membrane was rinsed in deionized (DI) water when PV experiments were completed for each condition. All tests were repeated for reproducible results and refill of liquid nitrogen was done to ensure constant level of liquid nitrogen throughout experiments. The trap was found to be effective at capturing flux, where initial tests showed good overall mass balance of the feed and permeate, and no more than 15% difference between the ammonia mass lost in the feed tank and the amounts captured in the permeate traps. However, the membrane performance was measured in terms of captured mass.

A series of pervaporation experiments for water-ammonia separation were conducted with synthetic feeds at various operating conditions. With a blank solution consisting of 500 mg/L sodium chloride (NaCl) and deionized (DI) water, two synthetic feed solutions with ammonia concentrations of 50 and 1000 mg/L were prepared by dissolving ammonium hydroxide (28–30% NH_3, Sigma-Aldrich) into the blank solution. The NaCl and ammonia concentrations were selected to broadly represent industry samples. The pH values of the two feeds were 10 and 11 at 25 °C, respectively for the two ammonia concentrations used. To ensure all ammonia was captured for analysis, during sampling a 1.0 wt % sulphuric acid (H_2SO_4) solution was added to the nitrogen traps to capture the ammonia in downstream (permeate side of the membrane) for product concentration analysis. The total nitrogen concentration (indicative of NH_3 concentration) of the feed and permeate samples was measured using the Total Nitrogen unit (Model no: TNM-1) of the Shimadzu TOC/TN analyser. All samples were diluted to a measurable level using DI water, *i.e.,* 0–50 mg/L. More measurement details can be found elsewhere [7].

To analyse the practical separation of the membrane, the apparent selectivity, β_{ij} *of* component i (ammonia) over j (water), was used. β_{ij} is a dimensionless parameter that looks at the overall separation accommodating both membrane selectivity and distillation separation effects that will be occurring in pervaporation systems. Here it is used to characterize the apparent selectivity of ammonia over water in pervaporation, as:

$$\beta_{ij} = \frac{(c_i/c_j)_p}{(c_i/c_j)_f} \approx \frac{(c_i)_p}{(c_i)_f} \tag{1}$$

Here, the subscript p is for permeate and subscript f is for feed. It is assumed that the ammonia is dilute in both the feed and permeate and thus $(c_j)_p \approx (c_j)_f$. Therefore, the simplified expression on the right hand side of Eq. (1) is applicable for dilute aqueous solution with low ammonia (i) concentration c_{NH_3} (mol or wt%).

The parameter β_{ij} is useful for understanding the overall separation of ammonia from water. However, since both ammonia and water are volatile, another parameter is needed that removes their individual distillation separating effect so the separation function of the membrane can be found. To reveal the intrinsic separation properties of the hybrid silica membrane, the permselectivity, α_{ij}, is used. It is defined as the ratio of the permeabilities or permeance of components i and j through the membrane, as [33]:

$$\alpha_{ij} = \frac{P_i^G}{P_j^G} = \frac{P_i^G/\ell}{P_j^G/\ell} \tag{2}$$

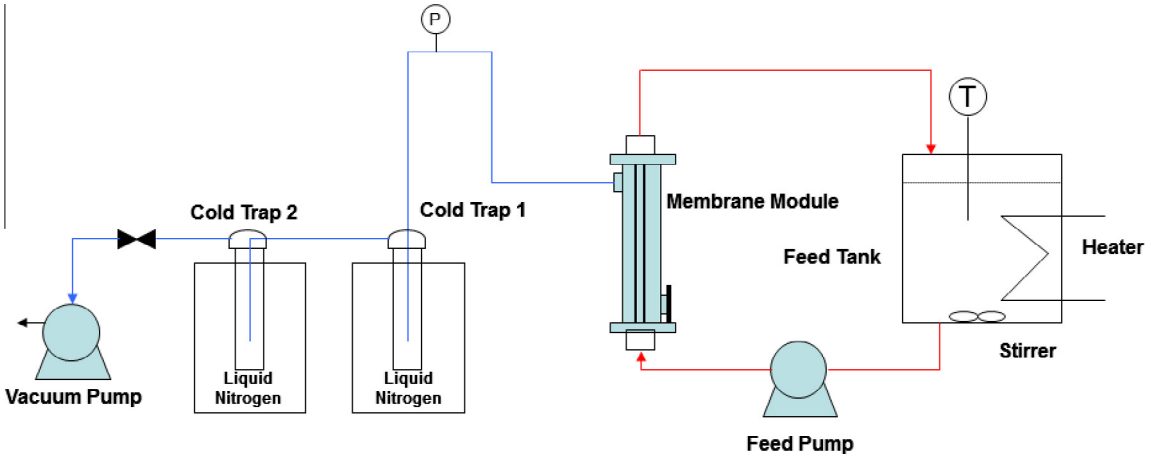

Fig. 1. Pervaporation experimental setup.

where P_i^G is the membrane gas permeability of component i (cm^3(STP)·cm/cm^2 s cmHg) and ℓ is the membrane thickness. P_i^G/ℓ is the permeance of component i. It can be defined as the component flux normalized for driving force across the membrane:

$$\frac{P_i^G}{l} = \frac{D_i K_i^G}{l} = \frac{J_i}{p_{io} - p_{il}} \approx \frac{J_t (c_i)_p}{p_{io}} \tag{3}$$

where D_i is the membrane diffusion coefficient (cm^2/s) of component i; K_i^G (cm^3(STP)/cm^3 cmHg) is the sorption coefficient. J_i is the molar flux of component i with unit of cm^3 (STP)/cm^2 s and J_t is the total flux. p_{io} and p_{il} are the respective partial pressure of the component i on either side of the membrane (surface o and ℓ). In pervaporation using vacuum on the permeate side, $p_{il} \ll p_{io}$, which leads to simplified form shown on the right hand side Eq. (3). Eq. (3) is valid for both the ammonia (i) and the water vapour (j). Substituting Eq. (3) into Eq. (2), α_{ij} can now be determined by:

$$\alpha_{ij} = \frac{(c_i/c_j)_p}{(p_{i0}/p_{j0})} \tag{4}$$

The partial pressure of the feed side, p_{io}, can be obtained based on Henry's law [33]:

$$p_{io} = H_{io} x_{io}^L \tag{5}$$

where H_{io} is the Henry's law constant [34] indicating the ammonia vapour-dissolved ammonium equilibrium relationship, x_{io}^L is the mole fraction of the component i in the feed liquid. In the dilute system, p_{jo} is simply the equilibrium vapour pressure of water. Eq. (4) represents a more convenient means to determine α_{ij} that does not rely on experimental flux data that can add additional errors to the calculated value. Interestingly, we can see the relationship between α_{ij} and β_{ij} if we substitute Eq. (1) into Eq. (4):

$$\alpha_{ij} = \beta_{ij} \frac{(c_i/c_j)_f}{(p_{io}/p_{jo})} \tag{6}$$

This shows that α_{ij} will vary according to β_{ij} in the same system, but will also be altered by conditions affecting p_{jo} and p_{jo} such as feed temperature. For the purpose of this investigation, β_{ij} (Eq. (1)) will be primarily utilised for analysing the separation performance, but α_{ij} will be calculated (Eq. (4)) for the purpose of discussing the role of the membrane in separating ammonia from water. As both β_{ij} and α_{ij} have the same subscript ij, indicating the separation between components i (ammonia) and j (water), in this paper simplified symbols β and α are used for discussions.

2.3. Material characterization

To correlate with the membrane performance, the membrane morphology was characterized as well as the material properties of each layer were analysed. Also, in order to explore the effect of the solutions on the materials, an extreme exposure test was conducted by immersing the films in various solutions prior to analysing their properties. Structure changes after alkaline solution treatment were studied. Specifically, the γ-alumina and hybrid silica materials were treated separately in 4.0 wt% ammonia solution with 500 mg/L NaCl for 72 h at room temperature; while the treatment in ammonia-free 500 mg/L NaCl solution was used for comparison. The high ammonia concentration relative to the membranes was chosen to represent the extreme exposure case representing the target concentration value for practical reuse of capture ammonia. Characterization was carried out on materials before and after solution treatments.

Scanning Electron Microscope (SEM) was used to characterize the intact and used hybrid silica membranes as well as the associated bulk materials from each layer. Membrane samples were prepared by fracturing pieces in the area of interest. The used membrane tubes were broken for post-experiment SEM images. Dried samples (membrane pieces or material powders) were mounted on special stubs and coated with a thin layer of gold under vacuum in a sputter coater (NeoCoater MP-19020NCTR). The cross-section and surface of the membranes were examined using a NeoScope JCM-5000 benchtop SEM. The crystalline structure of the γ-alumina bulk material representing the membrane interlayer was explored by X-ray diffraction (XRD), obtained via a PW3040/60 X'Pert PRO (PANalytical) diffractometer equipped with a Cu Ka radiation source (wavelength of λ = 0.15432 nm) and operated at 40 kV and 40 mA. The γ-alumina samples were ground to fine powder and packed uniformly onto a glass slide sample holder (2 mm × 3 mm) to create a flat upper surface. The XRD signals for intact and degraded γ-alumina structures were compared. The functional groups of the original and used hybrid silica materials (membrane top layer) were investigated by Fourier transform infrared spectroscopy (FTIR) with a Bruker equinox 55 at a resolution of 4 cm^{-1} and 32 scans in the wavelength range of 450–4000 cm^{-1}. Prior to testing, both the silica samples and KBr diluent (matrixes) were ground to fine powders, respectively. A small amount of silica powder was mixed with the KBr powder at a ratio of Silica: KBr of 1:500. The mixture was ground till homogeneous and pressed into transparent thin films for FTIR scanning.

The adsorption isotherms of membrane materials were measured via physical adsorption-desorption experiments, in pressures ranging from 0 to 100 kPa (absolute). N_2 adsorption using Tristar 3000 (Micromeritics, USA) was applied in determining the BET surface area, pore volume and pore size of the mesoporous γ-alumina film; while CO_2 adsorption using Tristar 3030 was to analyse the pore structure of the microporous hybrid silica layer due to pore size restriction (*i.e.,* relative pressure $p/p_0 < 0.03$, or 85.6 kPa for a saturation pressure of 5.73 MPa, for pore size smaller than 0.5 nm [35]). The solute concentration, e.g., Si and Al dissolving in the 4.0 wt% ammonia solution was determined by an Inductively Coupled Plasma Spectrometry (ICP) instrument E-9000, Shimazu. The respective calibration curves for Al and Si elements were obtained through measurement of standard solutions.

3. Results and discussion

3.1. Separation performance of hybrid silica membrane in ammonia solutions

To investigate the applicability of hybrid silica membranes in ammonia capture from aqueous solution, pervaporation experiments using membrane #1 were initially conducted using synthetic solution with low ammonia concentration of 50 mg/L and a natural pH of 10.0 at feed temperature of 45 °C, which was considered based on the available waste heat at various industry sites. The apparent selectivity of ammonia β (Eq. (1)) and total flux J in terms of operation time are given in Fig. 2. With a total flux stable at 4.3 kg m^{-2} h^{-1}, the ammonia is concentrated up to 12-fold (β = 12) during operation. This shows that the membrane effectively captured ammonia from the feed and would therefore work in a water treatment application. However because ammonia is already expected to preferentially distil over water due to its lower boiling temperature, permselectivity, α (Eq. (4)) was also explored in order to compare the performance against the distillation. The intrinsic permselectivity α of ammonia and water through the hybrid silica membrane was calculated as 0.5 based on Eq. (5). A value of 1.0 would be expected if the membrane did not contribute at all to the separation (e.g. by selective diffusion) and was instead working completely by distillation. However the value of 0.5 indicates selectivity of water over ammonia, and that the permeated

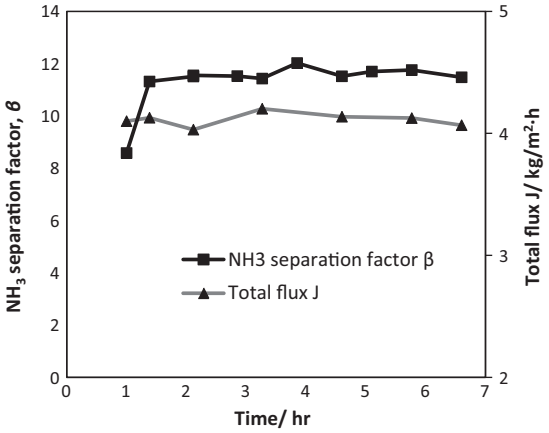

Fig. 2. Total flux J and NH_3 separation factor β of hybrid silica membrane #1 in low ammonia concentration (c_{NH_3} = 50 mg/L, T_f = 45 °C, Q_f = 500 mL/min, vacuum pressure = 0.3 ± 0.1 kPa absolute).

mixture is not better than what ideal distillation would produce as has been observed on other membranes during ethanol pervaporation [33]. This could also be due to the relatively low recirculating velocity (Reynolds number of 2300) employed in this work that led to poor mixing at the membrane surface and in turn significant temperature and concentration polarization effects that can alter the value of vapour pressure p_{io} assumed from vapour-liquid equilibrium. In our case, the hybrid silica membrane can engage in a molecular scale separation, where the transport mechanism of ammonia through the hybrid silica membrane could be hindered by size exclusion, but enhanced by adsorption selectivity [7,9]. Therefore while the hybrid silica membrane showed an ultimate ability to deplete the ammonia of the feed by capturing it at higher concentration, ammonia diffusion was limited due to hydrodynamics at the membrane surface and/or size exclusion in membrane pores. In any case, stable performance was observed but high concentrations and temperature will now be explored as this is where membrane degradation has been observed in past work [7].

The influence of feed temperature on the total flux and separation factor β (Eq. (1)) of the same hybrid silica membrane #1 at high ammonia feed concentration of 1000 mg/L is presented in Fig. 3. The vertical lines are used to separate different testing periods at varied feed temperature, *i.e.,* initially three temperatures 45, 50 and 70 °C were tested on day 1, day 2 and day 3–4, respectively; and then 45 tests were repeated on day 5 to compare with benchmark performance on day 1; lastly the PV experiments repeated at 70 °C from day 6 to day 10 were continuous testing without interruption. Compared to the flux results at 50 ppm (4.3 kg m^{-2} h^{-1}, Fig. 2), the initial flux of at 1000 ppm is lower at the same feed temperature of 45 °C, *i.e.,* 3.0 kg m^{-2} h^{-1} as shown in Fig. 3(a). This is consistent with our previous observation that the flux decreases with increasing ammonia concentration [7], which affects the water content in the solution. This can be due to the hindrance of water diffusion by the minor ammonia component, where effects such as competitive adsorption of more slowly diffusing large molecules occupying the micropores can block the total transport pathway. However, a general decreasing trend of total flux is observed at each temperature as shown in Fig. 3(a), varying from 45 to 70 °C, regardless of operating intervals. For

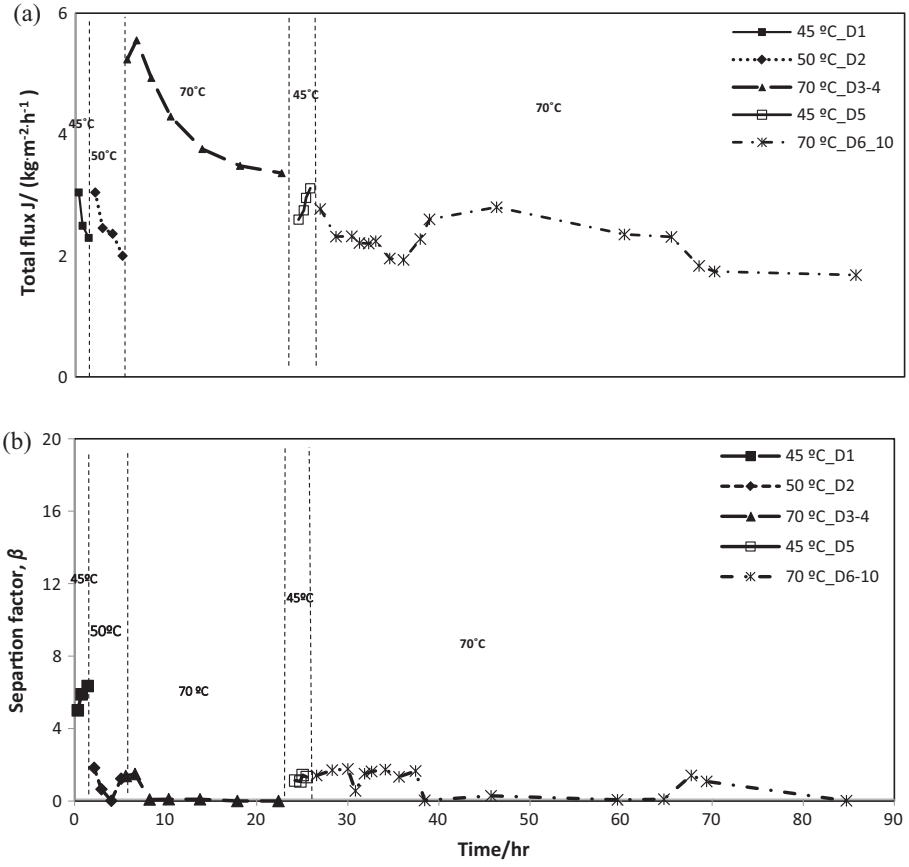

Fig. 3. Performance of hybrid silica membrane #1 in high ammonia concentration along operation time (a) Total flux J; (b) separation factor β (c_{NH_3} = 1000 mg/L, T_f = 45–70 °C, Q_f = 500 mL/min, vacuum pressure = 0.3 ± 0.1 kPa absolute).

instance, the initial tests at 45, 50 and 70 °C all showed major flux decline up to 50% in the first few hours. Especially at 70 °C, the silica membrane reaches a high flux up to 5.8 kg m^{-2} h^{-1} and then quickly drops to 3.36 kg m^{-2} h^{-1}, indicating of performance alteration at high temperature. A repeat test of this membrane at a low temperature of 45 °C on day 5 shows a slight increasing trend, which is contradictory to that of 45 °C test on day 1, suggesting change in membrane intactness. The results for a continuous operation from day 6 to day 10 repeating tests at 70 °C are also shown. Compared to the 70 °C test on day 3, a much lower initial flux of 2.7 kg m^{-2} h^{-1} and a gradual 40% decrease is observed over the testing period of day 6–10. This could be associated with the structure degradation of the membrane possibly due to the exposure to alkaline ammonia environment.

Correspondingly, Fig. 3(b) shows the apparent selectivity of ammonia β as a function of operation time at varied feed temperature. At low temperature range (e.g., 45 °C) the hybrid silica membrane (intact at the beginning of experiments) initially exhibits ammonia separation factor β of 5 and above, which is consistent with the finding for lower concentrations where ammonia diffused in preference shown in Fig. 2. However, β decreases dramatically to below 1 as the feed temperature increases. Also, the repeat test at 45 °C on day 5 was completely different from that of day 1. The β starts to fluctuate at high temperature 70 °C on day 3–4 and day 6–10, which corresponds to the flux fluctuation in Fig. 3(a). The complete change of β from above 1 to below 0.01 or lower indicated the loss to ammonia transport due to an increase in water permeation. Although the permselectivity α is not included in Fig. 3(b) due to its identical trend to β, it is a useful parameter to discuss as it compensates for relative volatility of ammonia and water, which is a function of the chosen temperature and concentration conditions. α values above unity indicate that a membrane has a role in selectively diffusing ammonia over water as opposed to selectivity based on distillation equilibrium where the membrane had no selective role. Based on Eq. (5), the α in this case (Fig. 3) has decreased from 0.5 for intact membrane (Section 3.1) to 0.20 at the end of the day-1 45 °C test and continuously down to 0.05 at the end of day-4 70 °C tests; while as an intrinsic parameter, the α value of an intact membrane working by distillation is expected to remain similar under the same flow conditions, regardless of concentration and temperature changes. Thus, it is possible that some fundamental material change has occurred causing the changes in membrane properties and eventually leading to a blockage of ammonia while still allowing water to transport. Overall, the hybrid silica membrane has seemingly become more water selective in the long run at high temperature and high ammonia concentration. However, severe fluctuations of both separation function and total flux have shown evidence of the membrane structure undergoing degradation. To confirm the observed degradation, a repeat PV test on a fresh hybrid silica membrane #2 was conducted under a specified feed temperature of 70 °C while other operating conditions remained constant. The comparison of initial and final flux as well as separation factor β of membrane #1 and #2 is presented in Table 1. The flux declined by 36% resulting in significant loss in selectivity (β) for membrane #2 tested over a shorter period of time (*i.e.,* 5 h). This has confirmed the deteriorating performance of the membrane observed under the same conditions as for membrane #1. Overall it could be attributed to the exposure of the hybrid silica membranes to relatively high ammonia concentration (*i.e.,* 1000 ppm) during experimental testing, which has not been reported in any open literature. Although γ-alumina interlayers is commonly used for fabricating silica membranes, it has a low hydrostability [36]. However, the molecular sieve organosilica membranes are known to be one of the most hydrothermally stable type for solvent dewatering under harsh conditions, in which water however is a minor component in solutions at neutral pH and high temperature [30]. Therefore, the slight degradation in structure observed in this work implies that water exposure is not severe enough to compromise membrane performance under conditions for the alcohol dewatering applications. Thus, as an important step to explore more suitable membrane materials for aqueous solution treatment, particularly for ammonia capture, the mechanisms governing the membrane integrity is worth further investigation through material characterization.

3.2. Membrane material investigation after ammonia exposure

The representative SEM pictures presented in Fig. 4 show the morphologies of the outer surface and the cross-section of the intact and used hybrid silica membrane. Fig. 4(a) shows the macroporous support of the new membrane, while Fig. 4(b) presents the cross section of the γ-alumina intermediate layer on top of the functional hybrid silica layer for the same new membrane. Correspondingly, the used membrane tubes were fractured to obtain post-experiment SEM images. Fig. 4(c)–(d) shows the morphological changes of the used silica membrane after the overall 1.5 months of periodic ammonia testing, particularly with high concentration solutions (up to 1000 mg/L). Clearly, compared to the outer surface of the new membrane (Fig. 4(a)), namely the α-alumina support, the surface of the used membrane is covered by gel like substance and possibly salt crystals at a magnification of 800× (Fig. 4(c)). Given that the membrane samples were sufficiently dry for SEM and the stability of alpha-phase alumina material, the gel like substance could be due to the dissolution and migration of the intermediate and surface layers. Further observation into the cross section of the membrane at 5000×, the boundary between the α- and γ-alumina layers of the used membrane starts to disappear (Fig. 4(d)). This is strong evidence of morphological change. Even the most stable hybrid silica layer is affected. Overall, the α-alumina support layer is considered mostly intact due to its superior durability in aqueous environment [37]. Comprehensive material characterization will be conducted in the following sections to identify the structural and chemical shifts of the degraded materials.

To explore the suitability of the hybrid silica membrane in alkaline ammonia solution treatment, representative SEM images were taken of the γ-alumina material before treatment, after treatment in 500 ppm NaCl, and after 4.0 wt% NH_3 (as well as 500 ppm NaCl) treatment as presented in Fig. 5(a)–(c). It is observed in Fig. 5(a) that the surface of the untreated material is relatively smooth at a magnification of 10,000×. The surface roughness increases

Table 1
Membrane performance of two hybrid silica membranes #1 and #2 (feed mixture: 1000 ppm ammonia solution, T_f = 70 °C, Q_f = 500 mL/min).

Membrane No.	Initial flux, kg m^{-2} h^{-1}	Final flux, kg m^{-2} h^{-1}	Initial separation factor β	Final separation factor β
#1 (15 h testing at 70 °C)	5.56	3.36	1.50	0.01
#2 (5 h testing at 70 °C)	5.97	4.40	2.74	0.20

Note: The full results of membrane #1 are presented in Figs. 2 and 3. Membrane #2 is a fresh hybrid silica membrane for confirming the performance deterioration under similar testing conditions.

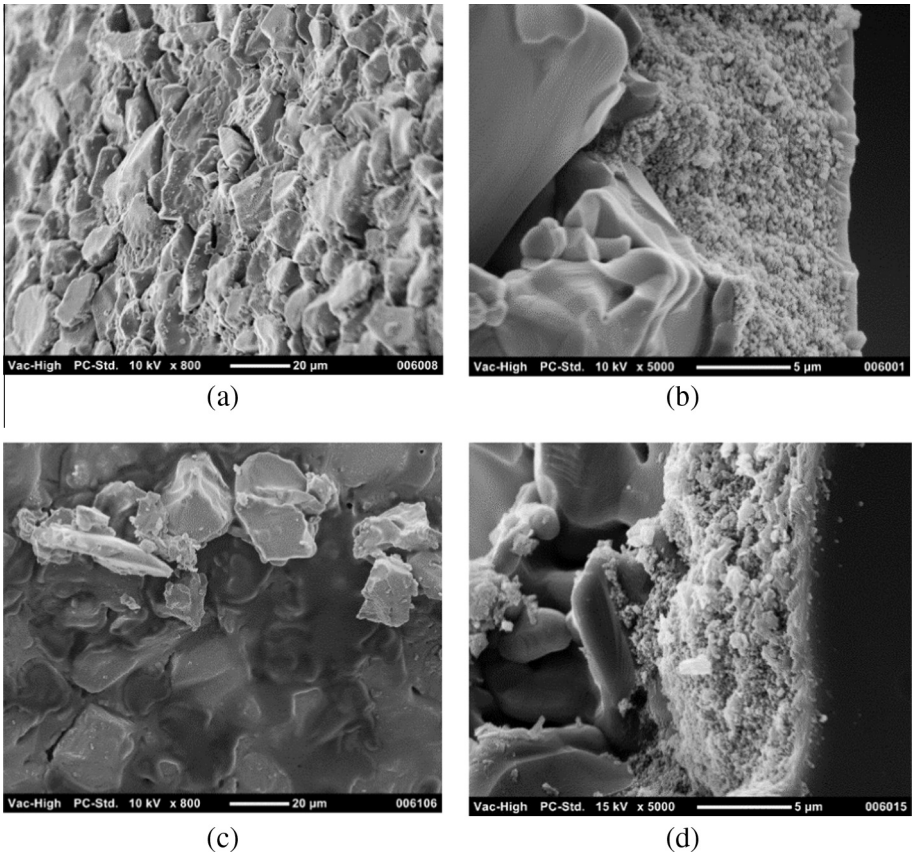

Fig. 4. Representative SEM images of hybrid silica before and after ammonia testing at high concentration shown in Fig. 3: (a) & (b) for outer surface and cross-section of original membrane; (c) & (d) for the same locations of used membrane.

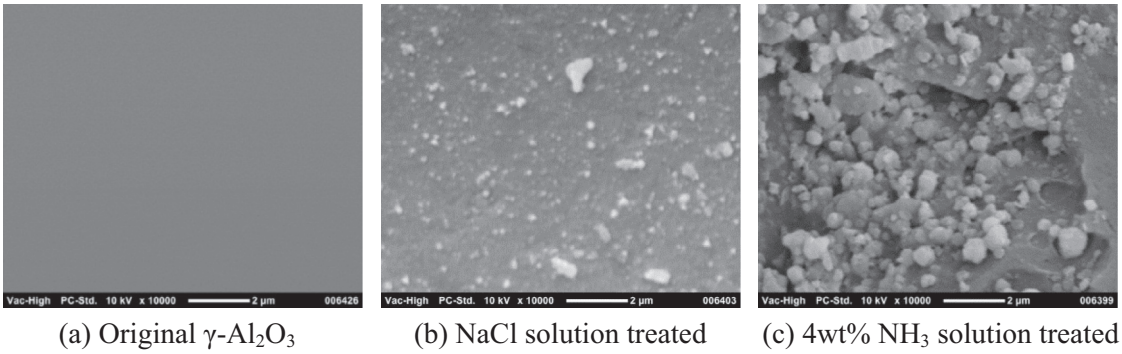

Fig. 5. Representative SEM images of γ-alumina film (as support layer of hybrid silica membrane) before and after solution treatments (a) for original film; (b) for 500 ppm NaCl solution treated film and (c) for 4.0 wt% NH_3 solution treated film.

slightly for the NaCl treated film. The surface appeared more rough after exposure, however the composition of the spots is unknown and therefore cannot be attributed to solids from solution (e.g. NaCl crystals) or degraded alumina. Regardless the structure did not undergone significant deterioration in this exposure condition, similar to reports on alumina published elsewhere [36], as shown in Fig. 5(b), no major morphological changes can be identified. As for the NH_3 solution treated γ-alumina film in Fig. 5(c), significant morphological changes are observed—large particles 100 µm in size and holes of 20 µm (observed on low resolution SEMs not shown here) with small particles of few hundred nm to 1 µm start to form in the material. The originally smooth and compact structure begins to disappear, which is consistent with the observation in Fig. 4(d). For the silica, slight cracking was observed at various locations on the smooth surface after the exposure to ammonia as shown in Fig. 6. Overall, fast material degradation of the γ-alumina layer and slight cracking of the hybrid silica layer in concentrated ammonia environment could contribute significantly to the deteriorating membrane separation function and fluctuating flux within such short operation time. However under the more extreme ammonia concentration for the materials test, it seems the γ-alumina interlayer degradation is the primary reason for the membrane performance degradation observed in Fig. 3.

Although the structural degradation of the γ-alumina intermediate layer as well as film material has been identified through morphological variation, it is important to investigate on the level of material characteristics and pore structure. Fig. 7 shows the comparison of the XRD patterns of the original and two treated

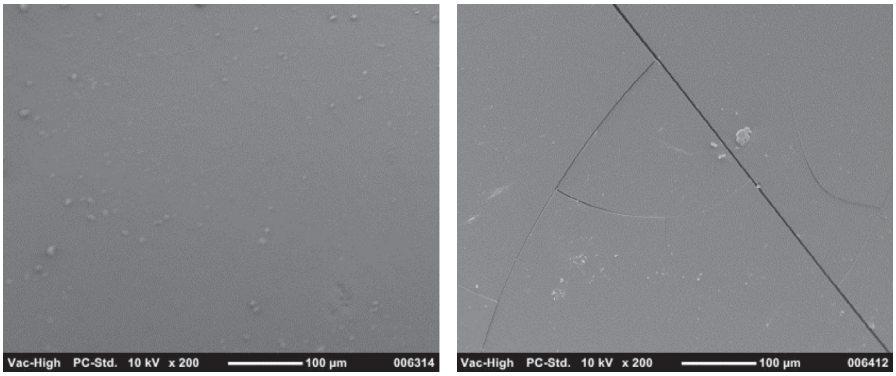

(a) Intact hybrid silica (b) 4.0 wt.% NH_3 solution treated

Fig. 6. Representative SEM images of hybrid silica film before and after NH_3 solution treatment (a) original (intact) film; (b) 4.0 wt% NH_3 solution treated film.

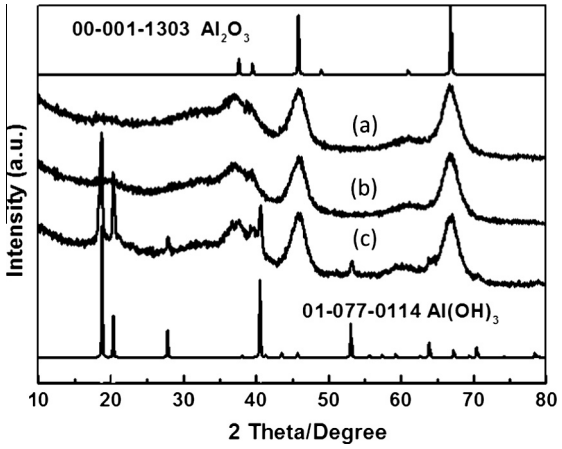

Fig. 7. XRD patterns of γ-alumina before and after 72-h solution treatments: (a) original film, (b) NaCl solution treated (c) 4.0 wt% NH_3 solution treated.

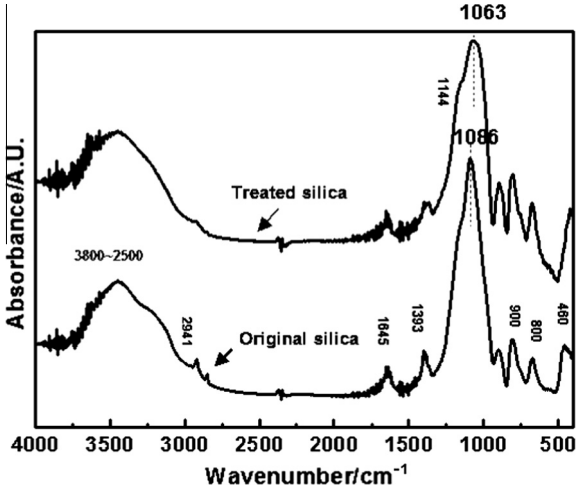

Fig. 8. FTIR spectra of hybrid silica film before and after solution treatment (top spectrum: original hybrid silica; bottom spectrum: 4.0 wt% NH_3 solution treated hybrid silica).

γ-alumina films. Clearly, the original γ-Al_2O_3 sample (spectrum (a)) presents a standard crystalline pattern, which has two primary Bragg peaks at 45.8° and 66.8° that are consistent with that obtained from the powder diffraction file (PDF card no. 00-01-1303), so as the treated sample with 500 ppm NaCl solution (spectrum (b)). However, for the NH_3 treated samples (spectrum (b)) the additional major Bragg peaks appearing at 2-theta of 18.7°, 20.3° and 40.5° have indicated the formation of $Al(OH)_3$, which also corresponds well to the standard pattern of $Al(OH)_3$ in the literature (PDF card no. 01-077-0114). Thus, the change of crystalline structure in the treated γ-alumina material could be explained through the hydration of γ-alumina phase in the NH_3 solution. According to prior studies, in which the membrane (as well as γ-alumina layer) remained stable in hydrothermal condition up to 190 °C [30], this current work has identified that the existence of NH_3 imposes significant influence on the phase change of the γ-alumina layer and results in hydrate formation. As the reaction of γ-Al_2O_3 and water is unlikely to take place at ambient conditions, we consider that ammonia acts as a catalyst for accelerating the conversion from Al_2O_3 to $Al(OH)_3$ and hence material degradation.

The FTIR results in Fig. 8 show the bands at wavelengths 460, 800 and 1086 cm^{-1} represent the vibrational modes of Si—O—Si. Particularly, the dominant band at 1086 cm^{-1} is assigned for the Si—O stretching. The vibration of silanol groups (Si—OH) appears at 900 cm^{-1}. The peaks at 2860 cm^{-1} and 2941 cm^{-1} correspond to the CH_2 symmetric and anti-symmetric stretching modes of polymer, respectively. A combined peak assigned to the surface silanols and hydroxyl groups appears between 3800 and 3000 cm^{-1}. Interestingly, subtle but clear changes can be observed from the spectrum of the NH_3 treated sample (top spectrum), where the dominant siloxane (Si—O—Si) peak shifts towards a lower frequency of 1063 cm^{-1}. Others have also attributed to the shift of wave number to slight structural movement of the silica network [38], suggesting slight change due to exposure to high strength ammonia. Moreover, the proportion of silanol to siloxane appeared to change slightly suggesting slight chemical changes of the silica. This could be explained through the hydrolysis of siloxane on the silica surface leading to the formation of silanol groups in alkaline ammonia environment. Previous work on silica has shown water exposure on reinforced structures leads to slight closures of small pores without compromising material integrity [16], which may explain the briefly observed high water selectivity over the larger ammonia molecules before the membrane seriously degraded (Fig. 3). Meanwhile ammonia undermined the silica layer by significantly deteriorating the alumina support layer. This conclusion will be further explored through physical adsorption, as discussed below.

Measurements of elements dissolved into solutions during liquid exposures helped to quantify the elemental changes in the treated solutions due to the solute dissolution from the solid materials. Gas porosimetry was also conducted to quantify the surface

Table 2
Dissolved concentration and its proportion of total mass of primary material elements, Si and Al, from respective membrane materials.[a]

Samples	500 ppm NaCl solution treatment		4% NH_3 + 500 ppm NaCl solution treatment	
	Si (ppm)	Al (ppm)	Si (ppm)	Al (ppm)
γ-alumina[b]	–	3.2 (<~0.01 wt%)[e]	–	14.0 (<~0.05 wt%)
Hybrid silica[c]	0.04 (4×10^{-5} wt%)[d]	–	2.1 (<0.002 wt%)	–
Hybrid silica[d]	–	–	4.2 (<0.004 wt%)	–

[a] Experimental error ±5%.
[b] γ-alumina was treated in both solutions for 72 h.
[c] Hybrid silica was treated in both solutions for 72 h (3 days).
[d] Hybrid silica was treated in both solutions for 1 month.
[e] Dissolution percentage to the total weight of sample treated.

Table 3
Results of gas adsorption experiments of membrane materials.[a]

Samples	Gas adsorption		
	N_2 BET[b], surface area (m^2/g)	CO_2 adsorption (mmol/g), @85.6 kPa	d_p, (nm)
γ-alumina	220	–	4.5
Treated γ-alumina[c]	210	–	5.9
Original hybrid silica power	210	1.85	–
Treated hybrid silica – 3 days[d]	200	1.79	–
Treated hybrid silica – 1 month[d]	170	1.69	–

[a] Experimental error ±5%.
[b] The data was processed by Brunauer, Emmett and Teller (BET) adsorption isotherm equation.
[c] γ-alumina was treated in 4%NH_3 solution for 72 h.
[d] Hybrid silica was treated in 4%NH_3 solution.

area and pore sizes of the γ-alumina and hybrid silica films before and after intensive exposure to ammonia, respectively. The results of dissolved mass of Al and Si and pore structure changes during solution treatments are given in Tables 2 and 3, respectively. For Al, the material loss was quantified as dissolution concentrations of 4.9 mg/L and 14 mg/L of Al in the treated NaCl and ammonia solutions, respectively, corresponding to between 0.01 and 0.05 wt% of the total sample mass in the first 72 h, as given in Table 2. Also, the elemental analysis of the liquid solution detected a dissolved Si concentration of 2.1 ppm in the treated ammonia solution after 72 h exposure (<0.002 wt%); while only 0.04 ppm (*i.e.*, $<4 \times 10^{-5}$ wt% material loss) was measured in the treated salt solution. Apparently, the dissolution of silica in the salt solution can be considered negligible compared to that in the ammonia solution highlighting the material stability in water under standard conditions. A continuous exposure to ammonia solution over 1 month period has resulted in an elevated dissolved Si concentration of 4.2 ppm (<0.004 wt%), which however is still one order of magnitude lower than the mass loss of the Al in alkaline ammonia solution. Overall, although the hybrid silica exhibited exceptional hydrothermal stability in alcohol dewatering [30], soluble Si on the surface and embedded in the framework may still dissolve in alkaline environment due to the non-uniform distribution of unstable Si—OH and stable Si—C—Si bonds. However the conditions in this test were much stronger than the maximum utilised in the membrane pervaporation presented in Fig. 3 (*i.e.* 1000 ppm).

BET surface area is a convenient technique to measure the porous property of a material, whereby changes in BET surface area indicate structural variation as reported elsewhere [16]. Therefore we have elected the same approach on materials to give evidence of the potential for the liquid solutions to degrade the same material that is responsible for the membrane selective property. In Table 3, the N_2 physical adsorption of the ammonia treated γ-alumina sample evidently shows that the pore diameter has increased from 4.5 to 5.9 nm in the first 72 h, resulting in an increased pore volume (based on classic cylinder model $d_p = 2\,V/A$) associated with widening pores and material loss. It coincides with the morphological changes (Fig. 5(c)), where the originally compact structure of γ-Al_2O_3 was attacked due to hydration during the simultaneous transport of ammonia and water through the membrane matrix. The material loss is confirmed by the elemental dissolution of Al as shown in Table 2. For the hybrid silica material treated by the same solution, both the BET surface area and adsorption amount (calculated based on CO_2 isotherm at absolute pressure of 85.6 kPa) drop with increasing treatment time, *i.e.*, from 214 m^2/g (CO_2 adsorbed: 1.85 mmol/g) to 170 m^2/g (CO_2 adsorbed: 1.69 mmol/g) after 1 month exposure to ammonia, indicating a decrease in micropore volume. The possible explanation is related to the reaction of water molecules with the structure and closing the pore volume as discussed earlier, which is supported by the observations of water selectivity prior to more significant degradation from the alumina layer. Pore loss can also be attributed to the migration of mobile silano-groups due to hydrolysis reaction and eventual blockage or collapse of small pores [13]. The evidence to silica structural degradation is further supported by the CO_2 adsorption curves over time, as shown in Fig. 9. However, only up to 9% decrease of the absolute absorption amount was observed over 1 month. Thus, no dramatic structural changes could be quantified through chemical/elemental and physical adsorption of the hybrid silica material. Nevertheless, it is obvious that the silica films became fragile with noticeable cracks (Fig. 7) at the extreme concentration condition, being much higher than the membrane test condition. These changes may still alter the performance of the membrane in application of ammonia separation at the lower concentrations, but due to the more significant impact to the alumina layer immediately below in the membrane, no strong conclusion can be drawn on the possible changes to membrane performance due to the hybrid silica layer.

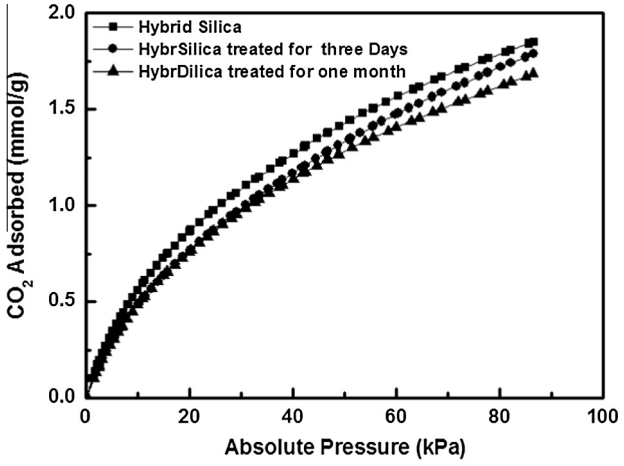

Fig. 9. CO_2 adsorption curves for original and treated hybrid silica samples at absolute pressure.

This work has shown that ammonia concentration from 50 ppm solutions is viable for ammonia separation, but at higher concentrations significant membrane degradation occurs. Interlayer free type silica membranes have already been developed [39,40]. Specifically, a hybrid silica membrane made by Pervatech similar to the one featured in this study but with an alternative interlayer (to replace the γ-alumina layer) is being developed to address this interlayer instability issue. In addition, future work on ammonia separation may include an engineered material with pore size that can accommodate ammonia molecules; while stability issues must be addressed to ensure long term performance.

4. Conclusions

This study has explored the potential of capturing or stripping ammonia from its aqueous solution for direct reuse through vacuum pervaporation process on hybrid silica membranes. Initially the hybrid silica membrane showed a preference towards ammonia transport at low concentration with a separation factor up to 12 at stable total flux over the test period of nearly 7 h. As ammonia concentration (pH) increased the membrane was initially ammonia selective as observed for low concentrations, but became water selective at high feed temperature. The subsequent significant flux decline and fluctuating separation selectivity suggested the alteration in membrane integrity for continuous operation. Characterization of the degraded membrane and associated organosilica and γ-alumina membrane materials revealed the cause of the significant performance change. Consistent with the morphological observation, additional $Al(OH)_3$ phase appeared in the crystalline structure of the γ-Al_2O_3 composing of the supporting intermediate layer of the membrane. The intermediate layer was altered due to the accelerated hydration reaction in alkaline environment. Physical adsorption was able to quantify the degradation of pore structure after intensive exposure to ammonia, where the γ-alumina showed an increased pore size. Slight porous structure changes of the hybrid silica were suspected to be from the migration of mobile silano-groups on the surface but did not show significant deterioration, at least as much as the underlying alumina supporting layer.

With the inherent advantages for capturing or stripping ammonia in terms of chemistry and structure, γ-alumina supported silica membranes still need to overcome stability barriers to ensure long term performance. This study has found that hydrostable silicas such as organic hybrid silica membranes may possess the material stability required, however future developments for related applications involving ammonia should focus on alternatives to, or more stable forms of, the supporting γ-alumina layer.

Acknowledgements

The following funding parties are gracefully acknowledged for funding this work: City West Water, Victoria, Australia, and Industry Postdoctoral Fellowship Scheme, Victoria University, Australia. The authors would also like to acknowledge Dr. Dana Martens from the University of Queensland and Dr. Wayde Martens from the Queensland University of Technology for their kind support in obtaining the CO_2 adsorption data. J.C. Diniz da Costa gratefully thanks the support given by the Australian Research Council Future Fellowship Program (FT130100405).

References

[1] M. Henze, P. Harremoes, J.l. Cour Jansen, E. Arvin, Wastewater Treatment: Biological and Chemical Processes, Springer, 2002. ISBN 978-3-540-42228-0.
[2] H.W. Paerl, Cultural eutrophication of shallow coastal waters: coupling changing anthropogenic nutrient inputs to regional management approaches, Limnol. – Ecol. Manage. Inland Waters 29 (3) (1999) 249–254.
[3] A. Foss, A.K. Imsland, B. Roth, E. Schram, S.O. Stefansson, Effects of chronic and periodic exposure to ammonia on growth and blood physiology in juvenile turbot (Scophthalmus maximus), Aquaculture 296 (1–2) (2009) 45–50.
[4] P.H. Liao, A. Chen, K.V. Lo, Removal of nitrogen from swine manure wastewaters by ammonia stripping, Bioresource Technol. 54 (1995) 17–20.
[5] D. Qu, D. Sun, H. Wang, Y. Yun, Experimental study of ammonia removal from water by modified direct contact membrane distillation, Desalination 326 (2013) 135–140.
[6] C.-K. Chiam, R. Sarbatly, Vacuum membrane distillation processes for aqueous solution treatment—a review, Chem. Eng. Process. 74 (2013) 27–54.
[7] X. Yang, T. Fraser, D. Myat, S. Smart, J. Zhang, J.C. Diniz da Costa, A. Liubinas, M. Duke, A pervaporation study of ammonia solutions using molecular sieve silica membranes, Membranes (Basel) 4 (1) (2014) 40–54.
[8] L.D. Tijing, Y.C. Woo, J.-S. Choi, S. Lee, S.-H. Kim, H.K. Shon, Fouling and its control in membrane distillation—a review, J. Membr. Sci 475 (2015) 215–244.
[9] M. Kanezashi, A. Yamamoto, T. Yoshioka, T. Tsuru, Characteristics of ammonia permeation through porous silica membranes, AIChE J. 56 (5) (2010) 1204–1212.
[10] R. Kreiter, M.D.A. Rietkerk, H.L. Castricum, H.M. van Veen, J.E. ten Elshof, J.F. Vente, Stable hybrid silica nanosieve membranes for the dehydration of lower alcohols, ChemSusChem 2 (2009) 158.
[11] M.C. Duke, S. Mee, J.C. Diniz da Costa, Performance of porous inorganic membranes in non-osmotic desalination, Water Res. 41 (17) (2007) 3998–4004.
[12] M. Elma, C. Yacou, D.K. Wang, S. Smart, J.C. Diniz da Costa, Microporous silica based membranes for desalination, Water 4 (2012) 629–649.
[13] R.K. Iler, The Chemistry of Silica:Solubility, Polymerization, Colloid and Surface Properties, and Biochemistry, Wiley, New York, 1979.
[14] S. Giessler, L. Jordan, J.C. Diniz da Costa, G.Q. Lu, Performance of hydrophobic and hydrophilic silica membrane reactors for the water gas shift reaction, Sep. Purif. Technol. 32 (1–3) (2003) 255–264.
[15] R. Leboda, E. Mendyk, Hydrothermal modification of porous structure of silica adsorbents, Mater. Chem. Phys. 27 (2) (1991) 189–212.
[16] M.C. Duke, J.C. Diniz da Costa, P.G. Gray, G.Q. Lu, Hydrothermally robust molecular sieve silica for wet gas separation, Adv. Funct. Mater. 16 (9) (2006) 1215–1220.
[17] J. Campaniello, C.W.R. Engelen, W.G. Haije, P.P.A.C. Pex, J.F. Vente, Long-term pervaporation performance of microporous methylated silica membranes, Chem. Commun. 7 (2004) 834–835.
[18] R.M. de Vos, W.F. Maier, H. Verweij, Hydrophobic silica membranes for gas separation, J. Membr. Sci 158 (1–2) (1999) 277–288.
[19] S. Giessler, J.C. Diniz da Costa, G.Q. Lu, Hydrophobicity of templated silica xerogels for molecular sieving applications, J. Nanosci. Nanotechnol. 1 (3) (2001) 331–336.
[20] N.K. Raman, C.J. Brinker, Organic template approach to molecular-sieving silica membranes, J. Membr. Sci 105 (3) (1995) 273–279.
[21] G. Xomeritakis, S. Naik, C.M. Braunbarth, C.J. Cornelius, R. Pardey, C.J. Brinker, Organic-templated silica membranes – I. Gas and vapor transport properties, J. Membr. Sci 215 (1–2) (2003) 225–233.
[22] C.X.C. Lin, L.P. Ding, S. Smart, J.C. Diniz da Costa, Cobalt oxide silica membranes for desalination, J. Colloid. Interf. Sci. 368 (1) (2012) 70–76.
[23] S. Battersby, T. Tasaki, S. Smart, B. Ladewig, S. Liu, M.C. Duke, V. Rudolph, J.C. Diniz da Costa, Performance of cobalt silica membranes in gas mixture separation, J. Membr. Sci 329 (1–2) (2009) 91–98.
[24] H.L. Castricum, A. Sah, R. Kreiter, D.H.A. Blank, J.F. Vente, J.E. ten Elshof, Hydrothermally stable molecular separation membranes from organically linked silica, J. Mater. Chem. 18 (18) (2008) 2150–2158.
[25] R. Xu, J.H. Wang, M. Kanezashi, T. Yoshioka, T. Tsuru, Development of robust organosilica membranes for reverse osmosis, Langmuir 27 (23) (2011) 13996–13999.
[26] D.W. Breck, Zeolite Molecular Sieves: Structure, Chemistry and Use, Wiley, New York, 1974, pp. 593–724.
[27] M.E. van-Leeuwen, Derivation of Stockmayer potential parameters for polar fluids, Fluid Phase Equilib. 99 (1994) 1–18.
[28] L. Liberti, Ion exchange advanced treatment to remove nutrients from sewage, in: L. Pawlowski (Ed.), Physicochemical Methods for Water and Wastewater Treatments, Elsevier, 1982.
[29] Y. Hirabayashi, Pervaporation membrane system for the removal of ammonia from water, Mater. Trans. 43 (5) (2002) 1074–1077.
[30] H.M. van Veen, M.D.A. Rietkerk, D.P. Shanahan, M.M.A. van Tuel, R. Kreiter, H.L. Castricum, J.E. ten Elshof, J.F. Vente, Pushing membrane stability boundaries with HybSi® pervaporation membranes, J. Membr. Sci 380 (1–2) (2011) 124–131.
[31] Rong Xu, Jinhui Wang, Masakoto Kanezashi, Tomohisa Yoshioka, T. Tsuru, Development of robust organosilica membranes for reverse osmosis, Langmuir 27 (2011) 13996–13999.
[32] H.L. Castricum, R. Kreiter, H.M. van Veen, D.H.A. Blank, J.F. Vente, J.E. ten Elshof, High-performance hybrid pervaporation membranes with superior hydrothermal and acid stability, J. Membr. Sci. 324 (1–2) (2008) 111–118.
[33] R.W. Baker, J.G. Wijmans, Y. Huang, Permeability, permeance and selectivity: a preferred way of reporting pervaporation performance data, J. Membr. Sci. 348 (1–2) (2010) 346–352.
[34] G.N. Lewis, M. Randall, Thermodynamics and the Free Energy of Chemical Substances, McGraw-Hill Book Co., Inc., New York, N. Y., 1923.

[35] L. Mukosha, M.S. Onyango, A. Ochieng, H. Kasaini, Development of better quality low-cost activated carbon from South African pine tree (Pinus patula) sawdust: characterization and comparative phenol adsorption, Int. J. Chem. Nucl. Mater. Metall. Eng. 7 (7) (2013).
[36] G. Lefèvre, M. Duc, P. Lepeut, R. Caplain, M. Fédoroff, Hydration of γ-alumina in water and its effects on surface reactivity, Langmuir 18 (20) (2002) 7530–7537.
[37] H.P. Hsieh, Inorganic Membranes for Separation and Reaction, Elsevier, 1996, p. 590.
[38] Alexandra Fidalgo, L.M. Ilharco, The defect structure of sol–gel-derived silica/polytetrahydrofuran hybrid films by FTIR, J. Non-Cryst. Solids 283 (2001) 144–154.
[39] M. Elma, D.K. Wang, C. Yacou, J.C. Diniz da Costa, Interlayer-free P123 carbonised template silica membranes for desalination with reduced salt concentration polarisation, J. Membr. Sci 475 (2015) 376–383.
[40] M. Elma, D.K. Wang, C. Yacou, J. Motuzas, J.C. Diniz da Costa, High performance interlayer-free mesoporous cobalt oxide silica membranes for desalination applications, Desalination 365 (2015) 308–315.